

Relationship Between Fluorescent and Vibronic Properties of Detonation Nanodiamonds and Strength of Hydrogen Bonds in Suspensions

A. M. Verval,† S. A. Burikov,† O. A. Shenderova,‡ N. Nunn,‡ D. O. Podkopaev,§ I. I. Vlasov,||,⊥ and T. A. Dolenko*,†,⊥

†Department of Physics, Moscow State University, 119991 Moscow, Russia

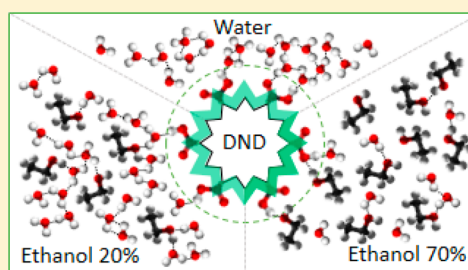
‡Adamas Nanotechnologies, Inc., 8100 Brownleigh Drive, Suit 120, Raleigh, North Carolina 27617 United States

§Moscow State University of Food Production (MSUFP), Volokolamsk Highway 11, Moscow, 125080 Russia

||General Physics Institute, Russian Academy of Sciences, Moscow, 119991 Russia

⊥National Research Nuclear University MEPhI, Kashirskoe Avenue 31, Moscow 115409, Russia

ABSTRACT: The use of detonation nanodiamond (DND) slurries in biomedical applications requires the understanding of interactions at the particle/solvent interphase. In this article, interactions of nanodiamond particles with molecules of protic solvents (water and water–ethanol mixture) were studied by the methods of laser Raman and fluorescence spectroscopy. It was found that nanodiamonds modified by carboxyl groups significantly decrease the average hydrogen bonds energy in protic solvents. In turn, the strength of hydrogen bonds at the DND/solvent interphase influences the fluorescent properties of nanodiamonds: the weaker the effect of the hydrogen bonds, the stronger is the fluorescence of DNDs in suspensions.



INTRODUCTION

Because of its unique properties, detonation nanodiamonds (DND) have wide perspectives in biomedical applications. Well-elaborated conjugation schemes of DND with biomolecules provide a solid background for their applications as fluorescence biomarkers and nanosensors.^{1–4} DND particles are also considered in targeted in vivo drug delivery^{5–9} and as a platform for immobilization of biomolecules.^{10,11} In the above and other biomedical applications of DND, they are used as slurries in biologically compatible media. In these applications, understanding of the processes at the nanoparticle/media interphase is imperative. As a first step, understanding of the interactions of surface molecular groups of DND with solvent molecules, particularly water molecules, and the structure of the DND/solvent interphase is required.

A wide variety of publications are devoted to suspensions of nanoparticles of CdSe/ZnS, SiC, SiO₂, Ag, and other nanomaterials in different solvents^{12–18} including water (SiO₂,¹⁵ Ag¹⁸). It was shown that the optical properties of nanoparticles can be significantly changed as a result of the interactions between nanoparticles and solvent molecules.^{14,15,17} Quenching of the fluorescence of CdSe and CdTe nanoparticles in water solutions was studied¹⁷ and it was demonstrated that the decrease of intensity of the electron exchange between particles and solvent depends on three factors: the distance between particles, the size of nanoparticles, and the direction of the electric field between nanoparticles created by their surface charges. In ref 15, it was demonstrated

that polarity of the solvent had significant influence on radiative properties of SiO₂ nanoparticles in water suspensions.

While the molecular interactions in suspensions of pointed nanoparticles have been extensively studied, and the nanophase of water has been discovered in nanodiamond gel 10 years ago,^{19,20} the interactions of the functional molecular groups of DND with solvent molecules require further investigation. The difficulties impacting progress in investigation of DND/solvent interactions are as follows. First, the methods of production of stable DND suspensions in water and the other solvents have been elaborated only recently.^{1,21–24} It should be noted that fabrication of stable DND suspensions is still a complicated problem and it requires further development of methods of preparations of such suspensions. Second, the polyfunctionality of a DND surface and wide variety of possibilities of surface functionalization with specific surface groups provide a large diversity of DND types to be studied.^{1–9,25,26}

The significant influence of DND dispersed in water on composition and characteristics of the solvent was demonstrated.^{27–35} The change of pH and concentration of oxygen in water suspensions was measured under the influence of increase of the concentration of DND modified by hydrogen.³⁰ This experiment demonstrated that the regular electron exchange between surface hydrogen of DND and water molecules (oxidation–reduction reaction $O_2 + 4H^+ + 4e^- = 2H_2O$) takes

Received: April 6, 2016

Revised: July 24, 2016

Published: August 2, 2016

place. It results in consumption or creation of O₂. This electron exchange influences such properties of suspensions as the angle of contact of water with the surface of nanodiamonds and the sign of charge on the nanodiamond surface. Because of the increase of electrostatic attraction as a result of the charge transfer, the ability of water films to adsorb on the ND surface increases. Using synchrotron X-ray scattering and absorption, the authors observed valence holes for oxidized DND in water.^{31–33} Their existence can be explained by electron transfer from the surface of dispersed DND to surrounding water. The electron transfers can influence colloidal, optical, chemical, and catalytic properties of DND in water. The influence of the interactions of DND with solvent molecules on the optical properties of DND was studied in ref 34 and 35 with the help of laser Raman and fluorescence spectroscopy. The DND fluorescence spectra in suspensions and the change of position and shape of the Raman stretching band of water³⁴ or OH-groups (in the protic solvents³⁵) were studied simultaneously. Earlier, it was demonstrated numerous times that the Raman stretching band of vibrations of OH-groups is very sensitive to any change of hydrogen bonds^{36–39} including the changes caused by the presence of different admixtures in water.^{36,37,40,41} As a result of quantitative analysis of changes of characteristics of water Raman stretching bands, it was found that DND in water suspension influences the structure of the surrounding water layer changing the strength of hydrogen bonds between water molecules. Moreover, different surface functional groups of DND change the strength and dynamics of hydrogen bonds in a different way.³⁴ In ref 35, it was shown that polarity of a solvent strongly influences the DND fluorescence: the greater the polarity of a solvent is, the weaker the fluorescence of DND in the suspension is. It was demonstrated that a change of fluorescent properties of DND in ethanol under heating can be caused by the change of the surface groups of DND due to interactions of ethanol molecules with initial functional groups of ND.⁴²

The purpose of this study was research of the mutual influence of dispersed DND modified by the carboxylic groups (DND–COOH) and the protic solvents on the properties of each other. One of the tasks was investigating the change of strength of hydrogen bonds of solvents as a result of interactions of DND surface groups with molecules of the solvents. For the first time, the evaluation of energy of hydrogen bonds that are not substantially changed by DND–COOH, is given. Another task was investigation of the influence of the solvent hydrogen bonds strength on the fluorescent properties of DND–COOH. The conclusion about interrelation of the strength of hydrogen bonds in the solvent and the intensity of DND–COOH fluorescence was confirmed. To solve these problems, solvents differing by strength and quantity of hydrogen bonds were modeled—water and water–ethanol solutions. The studies were conducted using fluorescence and Raman spectroscopy.

■ EXPERIMENTAL SECTION

Experimental Setup. Size of nanoparticles in the suspensions was measured by the method of DLS (analyzer “Zetatrac”, Microtrac).

Spectra of IR absorption were obtained using Varian 640-IR FTIR spectrometer (Resolution 4 cm⁻¹, ATR attachment with the ZnSe crystal).

Raman spectra of suspensions of nanodiamonds in water and water–ethanol solutions were measured using a laser Raman

spectrometer. For excitation, an argon laser (488 nm, power 250 mW, power density in cuvette 10 W/cm²) was used. Integral spectra were measured in a 90° scattering geometry. The system of registration consisted of a monochromator (Acton 2500i, focal length 500 mm, grade 900 grooves/mm) and CCD-camera (Horiba Jobin Yvon, Synapse 1024 × 128 BIUV, width of entrance slit 25 μm, resolution 2 cm⁻¹). The spectra were corrected to the power of laser radiation, spectrum accumulation time, and the spectral and channel sensitivity of the receiver.

Excitation of the fluorescent signal of solutions and ND suspensions was performed by blue diode laser (wavelength 405 nm, power 50 mW). Integral spectra were measured in a 90° geometry with the help of a monochromator (Acton 2500i, focal length 500 mm, grade 1800 grooves/mm) and PMT (Hamamatsu H8259-01). The width of the entrance and exit slits was 500 μm (it provided a resolution 0.5 nm). Spectra were measured in the region 410–750 nm.

A thermostabilizing system allowed setting up and controlling the temperature of the sample with an accuracy of 0.1 °C.

Materials. Preparation of DND Suspensions. DND modified by carboxyl groups (DND–COOH) have been studied because according to numerous publications^{3,43} these functional groups provide maximal biocompatibility of the nanoparticles. The initial DND were synthesized by detonation of a mixture of trinitrotoluene (TNT) and 1,3,5-trinitrotoluene-1,3,5-*x*-triazine (RDX) in media with water cooling (“New Technologies”, Chelyabinsk, Russia). Further purification from soot and treatment of DND were performed at Adámas Nanotechnologies (Raleigh, North Carolina). The procedures used were described in detail.⁴⁵ The modification of purified DND by COOH groups was carried out by means of thermal treatment of DND in air at 420 °C for a period of 1 h followed by purification in HCl. Primary characterization of similar samples was performed at the International Technological Center.^{44–46}

In our study for the preparation of the suspensions of DND–COOH in protic solvents, the initial water suspension of DND–COOH with concentration of 28 g/L was used.

To study the influence of dispersed DND–COOH and solvents on the properties of each other, several model solvents with different hydrogen bond strength were prepared. The selection was based upon the fact that in water–ethanol solutions at an ethanol concentration of approximately near 20 vol % self-organization of ethanol and water molecules is observed. It leads to amplification of hydrogen bonds in the solution in comparison with pure water (the effect of stabilization of the water structure).^{47–51}

Authors of some papers suppose that at this concentration the molecules of ethanol and water form clathrate-like structures. Ethanol molecules are located inside a shell of water molecules making this shell stronger and ordered.^{48,50} In a water–ethanol solution with an ethanol concentration of 70 vol %, the hydrogen bonds are, on the contrary, much weaker in comparison with those in pure water. These results were obtained both in theoretical calculations and during study of the water–ethanol solutions using calorimetric methods, NMR, FTIR, and Raman spectroscopy.^{47–51} Estimations of the energy of hydrogen bonds in water and water–ethanol solutions with ethanol concentrations of 20 vol % and 70 vol % have been performed.⁵² Enthalpy of hydrogen bonds in the specified solutions was $\Delta H^w = (-21.4 \pm 0.7)$ kJ/mol, $\Delta H^{20\%} =$

(-24.5 ± 0.8) kJ/mol, and $\Delta H^{70\%} = (-16.2 \pm 0.8)$ kJ/mol, respectively. Thus, by changing the concentration of ethanol in water one can model the media with different hydrogen bond strengths.

In this work, DND-COOH suspensions with a concentration of DND of 2 g/L were prepared in water and water-ethanol solutions with concentrations of ethanol of 20 vol % and 70 vol % (further -20% to 70%). Deionized water with an electrical conductivity of $0.1 \mu\text{Sm/cm}$ and alcohol with ethanol content of 96%, (Sigma-Aldrich) were used. The initial water suspension of DND-COOH with particle size of 10 nm, DND concentration of 28 g/L, and ζ -potential of -45.28 ± 11 mV was stable over a period of one year (time of observation).

Particle sizes in the obtained suspensions were measured using dynamic light scattering (DLS). According to the results of the measurements shown in Table 1, there are two types of

Table 1. Size of Particles of DND-COOH in Water and Water-Ethanol Suspensions with DND Concentration 2 g/L (Temperature 25 °C)

sample	solvent	small size/large size, nm	fraction of particles with small size, %	fraction of particles with large size, %
DND-COOH, 2 g/L	water	$10 \pm 2/35 \pm 3$	91.1	8.9
	ethanol 20%	$10 \pm 2/35 \pm 3$	91.9	8.1
	ethanol 70%	$11 \pm 2/40 \pm 3$	96.3	3.7

particles in the suspensions: prevalent particles with size 10–13 nm and a small amount of particles with size 35–40 nm. With increasing temperature of DND-COOH water suspension up to 55 °C the fractions of small and large particles changed within the limits of accuracy of the method (by 3–4%).

To control the stability of the functional layer of the DND-COOH IR absorption spectra were obtained for the DND-COOH samples that were dried from the initial water suspension with DND concentration 28 g/L (Figure 1a) and for the DND-COOH samples that were dried from suspensions in water and water-ethanol solution (20% of ethanol) with a DND concentration 2 g/L (Figure 1b). One can see from Figure 1 that on the surface of all samples the carboxyl groups dominate; in the spectral region of $1050\text{--}1100 \text{ cm}^{-1}$ and $1350\text{--}1500 \text{ cm}^{-1}$, there are vibrational bands of CO groups and in the region of $3000\text{--}3900 \text{ cm}^{-1}$ there are vibrational bands of OH groups. A broad band with maxima near 1110 and 1240 cm^{-1} is a typical characteristic of a DND sample and consists of a superposition of many lines: C—O—C, CH, C—C, and so forth. Therefore, the dispersion of DND-COOH in water-ethanol solvent did not alter the composition of the functional groups on the surface of nanodiamonds. Some discrepancies in the spectra are caused by inhomogeneous drying DND-COOH from suspensions.

RESULTS AND DISCUSSION

Temperature Dependencies of Raman Spectra of ND Suspensions. In this study, the temperature dependencies of Raman spectra of water and water-ethanol suspensions of DND-COOH with ethanol concentrations of 20 and 70% and Raman spectra of initial solvents (without DND) were obtained. Temperature was changed from 0 to 80 °C in increments of 5 °C. For example, in Figure 2 one can see the temperature dependencies of Raman spectra of water (Figure 2a) and water suspension of DND-COOH (Figure 2b); in Figure 3 the same dependencies for water-ethanol solution with concentration of ethanol 20% (Figure 3a) and for DND-COOH suspension in this solution (Figure 3b) can be seen.

As can be seen in Figure 2, changes of temperature leads to changes of bands of water intramolecular vibrations, the stretching vibrations of O—H ($3000\text{--}3800 \text{ cm}^{-1}$) and the

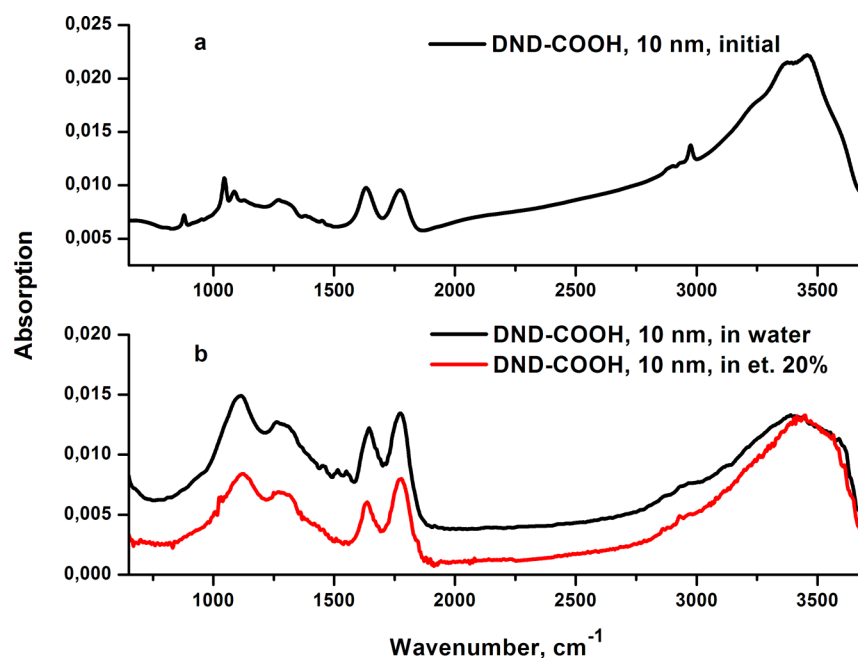


Figure 1. IR absorption spectra of DND-COOH powder dried from initial sample in water (a) and from suspensions in water and water-ethanol (20%) mixture (b).

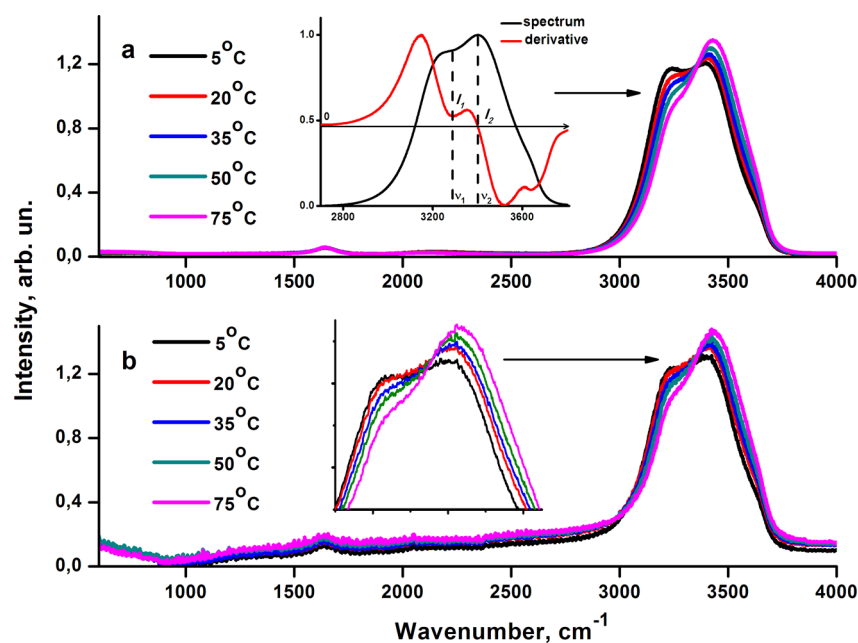


Figure 2. Raman spectra of water (a) and water suspension of DND–COOH (2 g/L) (b) at different temperatures. In the inset in panel a, one can see the illustration of calculation of the parameter $\chi_{21} = I_2/I_1$.

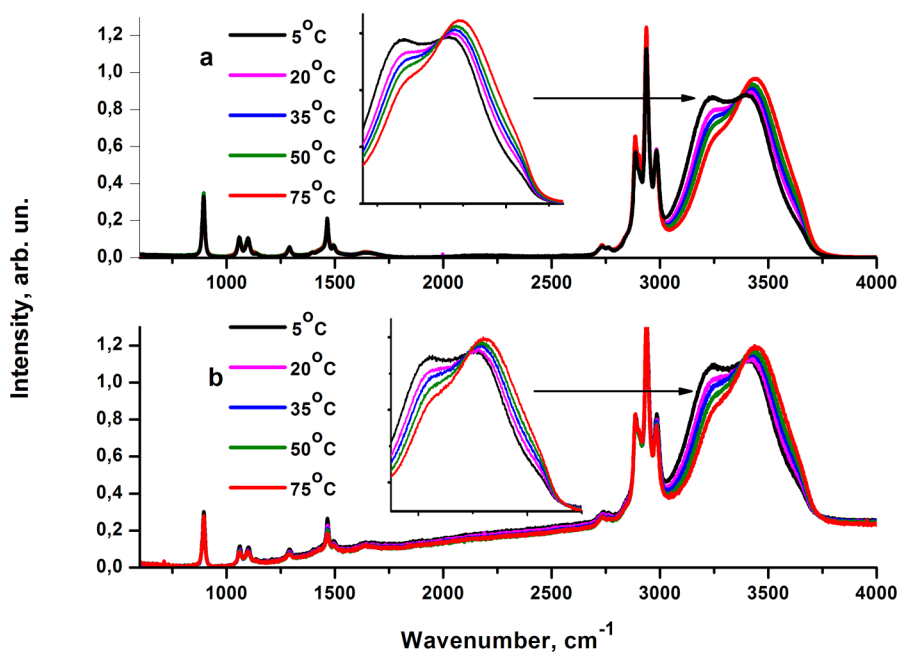


Figure 3. Raman spectra of water–ethanol solution with concentration of ethanol 20% (a) and of the suspension of DND–COOH (2 g/L) in this solvent (b) at different temperatures.

bending vibrations of H–O–H (with the maximum near 1600 cm^{-1}).

With decreasing temperature, the intensity of the high-frequency region of the stretching band decreases, the maximum of band shifts to low frequencies, and the half-width increases.^{36–40} Increase of temperature leads to increase of the intensity of the bending band. Such temperature dependencies of Raman spectra are well-known in literature and can be explained as follows.^{36–40} With decreasing temperature, the average energy of hydrogen bonds in water becomes lower, and the frequency of stretching vibrations of O–H decreases; this is why the stretching band shifts to low

frequencies and the intensity of low-frequency region of band increases.^{36–40}

To analyze the change of the average energy of hydrogen bonds in water using Raman spectrum the authors of this study suggested the use of quantitative characteristics of stretching bands as the ratio of the intensities of high-frequency and low-frequency regions of the stretching band (Figure 2a) $\chi_{21} = I_2/I_1$ and the shift of mass center.^{39–41} As it was calculated using temperature dependence of water Raman stretching band,⁵² the average energy of hydrogen bonds in water is equal to -21.4 kJ/mol. Assuming that the high-frequency region of stretching band (with maximum 2 and intensity I_2 , Figure 2a) is caused by

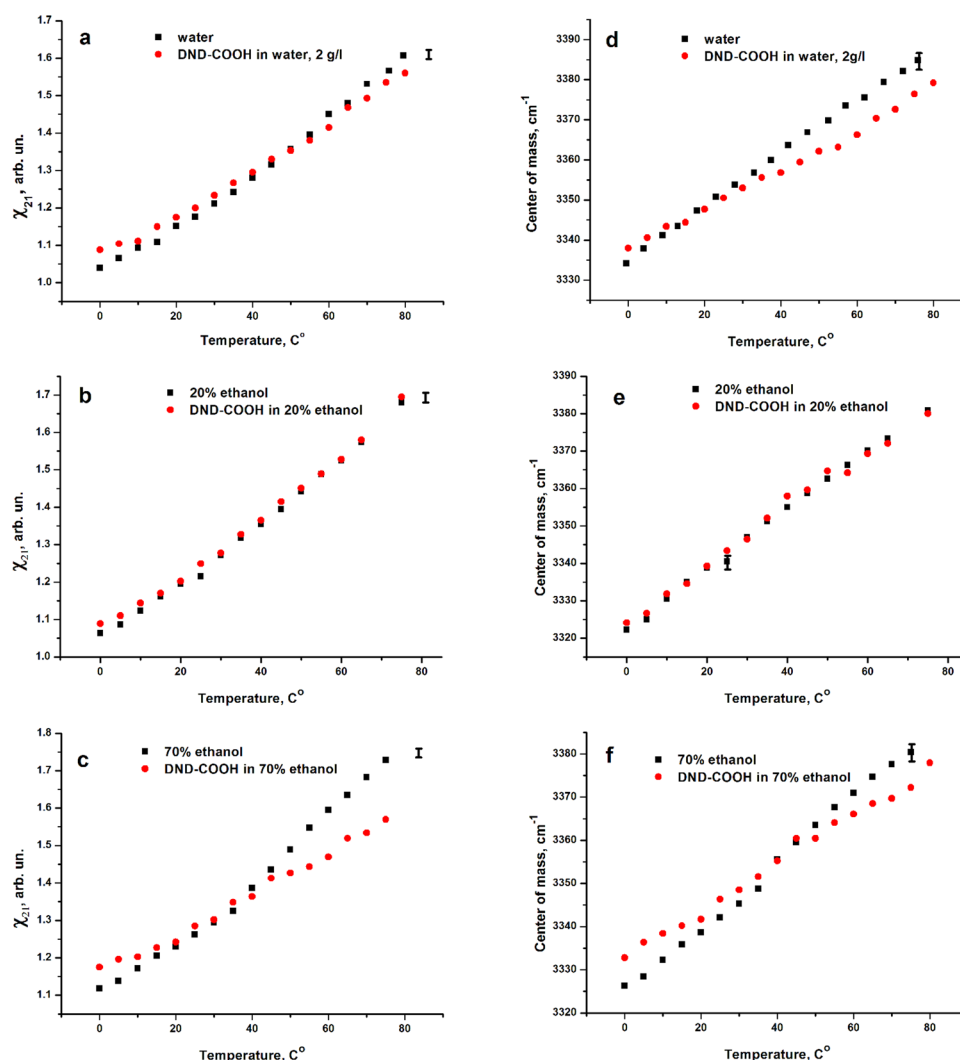


Figure 4. Temperature dependencies of parameters of stretching bands of OH groups for pure solvents and DND–COOH suspensions (DND–COOH concentration is 2 g/L).

vibrations of hydroxyl groups with weak hydrogen bonds and the low frequency region (with maximum 1 and intensity I_1) caused by vibrations of groups with strong hydrogen bonds, then the parameter χ_{21} characterizes the ratio of fractions of OH groups with weak and strong hydrogen bonds. Therefore, the increase of χ_{21} means the decrease of the average energy of hydrogen bonds in water, that is, decrease of quantity of hydrogen bonds with energies about $| -21.4 |$ kJ/mol. Figure 2a illustrates the calculation of χ_{21} : the points 1 and 2 are chosen according to singular points of the first derivative of the stretching band. Similar reasoning allows us to tell that the greater the shift of the center of mass of stretching band ν_{cm} to higher frequencies, the weaker the hydrogen bonds in water.

It should be noted that as a result of changes of temperature of water–ethanol solutions (Figure 3a), significant changes occur in the stretching and bending bands of vibrations of hydroxyl groups. Vibrational bands of molecular groups of ethanol—the bands of stretching vibrations C–C (886 cm⁻¹), of stretching vibrations C–O (1050 cm⁻¹), of torsion vibrations CH₂ (1270 cm⁻¹), of bending vibrations CH₃ and CH₂ (1440–1455 cm⁻¹), of symmetric stretching vibrations CH₂ (2880 cm⁻¹), of symmetric stretching vibrations CH₃ (2930 cm⁻¹), of asymmetric stretching vibrations CH₃ (2980 cm⁻¹) undergo

little changes in the intensity. It can be explained by the fact that in water–ethanol solutions the hydrogen bonds are formed mainly by hydroxyl groups. In Figures 2b and 3b one can also see the broad fluorescence bands of DND–COOH.

For stretching bands of all DND suspensions, the temperature dependencies of the center of mass ν_{cm} and the parameter χ_{21} were calculated. These dependencies are shown in Figure 4. The errors of determination of the frequency of the mass center and of the value of parameter χ_{21} are 3 cm⁻¹ and 0.02 (arbitrary units), respectively.

In Figure 4a–c, one can see that in all studied solutions and suspensions of DND with increasing temperature the parameter χ_{21} increases (that is, the average energy of hydrogen bonds in the solutions and suspensions become higher). However, the behavior of dependencies $\chi_{21}(T)$ demonstrates that in DND–COOH suspensions in water (Figure 4a) and in water–ethanol solutions with 70% of ethanol (Figure 4c), the decrease of the average energy of hydrogen bonds is caused not only by temperature increase but also by the presence of DND–COOH. The intersection of dependencies $\chi_{21}(T)$ for solvent and for suspension of DND–COOH in this solvent at temperature 50° (Figure 4a,c) supports this conclusion.

Therefore, nanodiamonds in the solution interact with the solvent molecules, reconstruct, and weaken the surrounding network of hydrogen bonds.¹² Around DND–COOH in water, the “hydrate shell” is formed, which is the layer of water molecules that form hydrogen bonds with surface groups COO[−] (with high probability hydrogen atom from carboxylic group transfers to water). The presence of two oxygen atoms with high electronegativity in carboxylic group causes strong polarization in this group. Because of this polarization, the groups COO[−] form more strong hydrogen bonds with water molecules in comparison with hydrogen bonds between water molecules themselves. In the other bulk water, molecules are also reoriented and network of hydrogen bonds becomes more “loose”. Exactly because of arising “looseness” of hydrogen bonds in the bulk of water, the value of parameter χ_{21} for pure water is lower than that for water DND–COOH suspension at the same temperature. With temperature increase, the average energy of hydrogen bonds in the bulk of water and in both DND–COOH suspensions and in pure solvent is decreased, which is why the parameters χ_{21} both in suspension and in pure water increase. However, the parameter χ_{21} for pure water increases faster than the parameter χ_{21} for DND–COOH suspension because in DND–COOH suspensions there are more strong hydrogen bonds than that in bulk of water. As a result, at temperature near 55 °C (Figure 4a) the parameter χ_{21} for pure water becomes higher than χ_{21} for water DND–COOH suspension; under the same heating (we mean the heat at constant temperature, necessary to change the average energy of hydrogen bonds for the same value) in pure water, the total decrease of the average energy of hydrogen bonds was greater than in suspensions because it required the greater amount of heat for weakening stronger hydrogen bonds around nanoparticle. Similar behavior is observed in the dependencies of the center of mass of stretching bands $\nu_{cm}(T)$ on temperature for the investigated samples (Figure 4d,f).

Thus, the comparative analysis of the obtained temperature dependences of the quantitative characteristics of stretching bands of OH groups in water and water–ethanol solution with ethanol concentration 70% and DND–COOH suspensions in them have demonstrated that the presence of nanodiamonds in the solvent leads to the decrease of the average energy of hydrogen bonds and destruction of hydrate structures. In this case, the energy of hydrogen bonds in DND–COOH suspensions in water and water–ethanol solution with 70% of ethanol becomes on average less than |−21.4| and |−16.2| kJ/mol, respectively. In the behavior of the dependencies, it is revealed as the intersection of the curves $\chi_{21}(T)$ and $\nu_{cm}(T)$ for DND–COOH suspensions and pure solvents.

However, for the water–ethanol solution with ethanol concentration 20% the dependencies, $\chi_{21}(T)$ and $\nu_{cm}(T)$ show another behavior (Figure 4b,e): throughout the range of temperature change the dependences of mentioned parameters for DND–COOH suspensions practically coincide with the corresponding dependencies for the pure solvent. There is no intersection of the curves. It means that suspended DND–COOH cannot weaken the hydrogen bonds with average energy |−24.5| kJ/mol in the solvent. Only one factor causes the decrease of average energy of hydrogen bonds: the temperature increase. Recall that just in water–ethanol solution with concentration 20% of ethanol one can observe the effect of strengthening of the hydrogen bonds in comparison with the hydrogen bonds in pure water.⁵² Thus, DND–COOH in the mentioned solvent cannot destroy stable hydrate compositions

with strong hydrogen bonds with average energy |−24.5| kJ/mol.

Thus, in the described part of the work to study the influence of DND–COOH on the hydrogen bonds in the suspensions we simulated environments with different strengths of hydrogen bonds. It turned out that DND with surface carboxylic groups are able to break the network of hydrogen bonds with an average energy |−21.4| kJ/mol but nearly do not weaken hydrogen bonds with average energy |−24.5| kJ/mol at room temperature.

Fluorescence Spectroscopy. In this work, the study of influence of the hydrogen bonds in the solvents on the fluorescence of dispersed DND–COOH was carried out. For this purpose, the spectra of fluorescence of DND–COOH in water–ethanol solutions with ethanol concentrations from 0 to 70% in increments 5–10% were obtained at constant temperature (25 ± 0.2) °C. The concentration of DND–COOH was 2 g/L in all suspensions. Fluorescence spectra of DND–COOH in water–ethanol solutions with different concentrations of ethanol are presented in Figure 5.

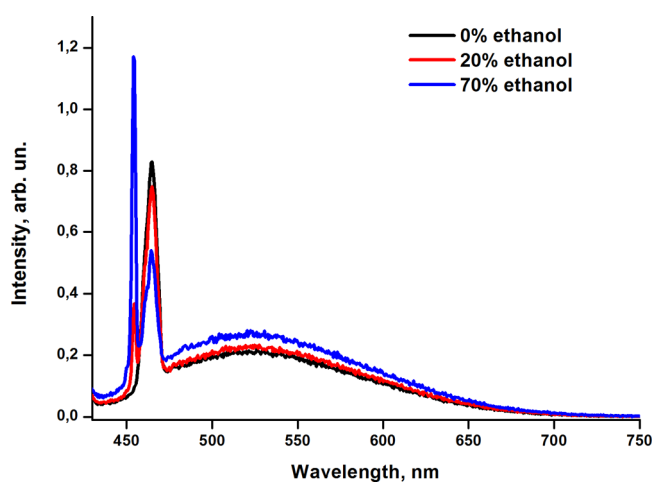


Figure 5. Raman and fluorescence spectra of DND–COOH suspensions in water–ethanol solutions with different concentration of ethanol. Spectra were normalized by the square of the Raman band of vibrations of OH and CH groups.

As a quantitative characteristic of the intensity of DND–COOH fluorescence, the parameter $F_0 = S_{FL}/S_{RS}$ was used. It is equal to the ratio of integral intensity of fluorescence to integral intensity of Raman stretching bands of OH and CH groups. The calculation of F_0 is illustrated in Figure 6 for the spectrum of fluorescence of DND–COOH in water and in Figure 7 for the spectrum of DND–COOH fluorescence in water–ethanol solution with concentration of ethanol 40%.

For correct comparison of the parameters F_0 of DND–COOH fluorescence in water and water–ethanol solvents, it is necessary to find an external benchmark that is not connected with the integral intensity of DND–COOH fluorescence and the integral intensities of stretching vibrations of OH and CH groups. However, the addition in the solution of another admixture (except studied substances) can essentially change the hydrogen bonds in the solution and influence the properties of nanodiamonds. That is why the spectra were normalized by the ratio of the integral intensity of stretching band of OH groups of water suspension of DND–COOH to the integral

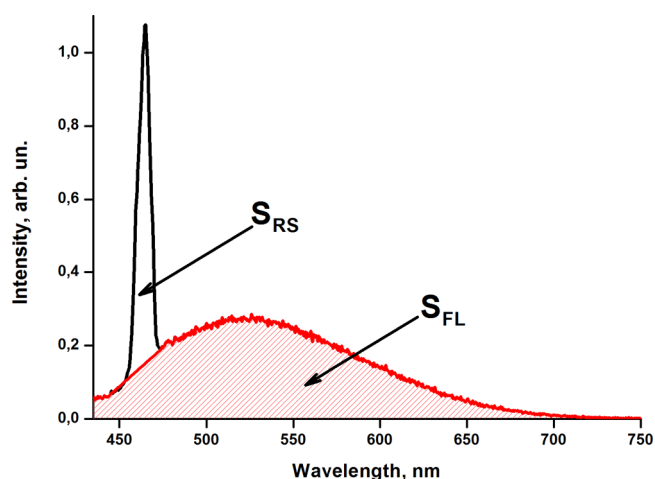


Figure 6. Fluorescence spectrum of DND-COOH in water. Illustration of calculation of F_0 .

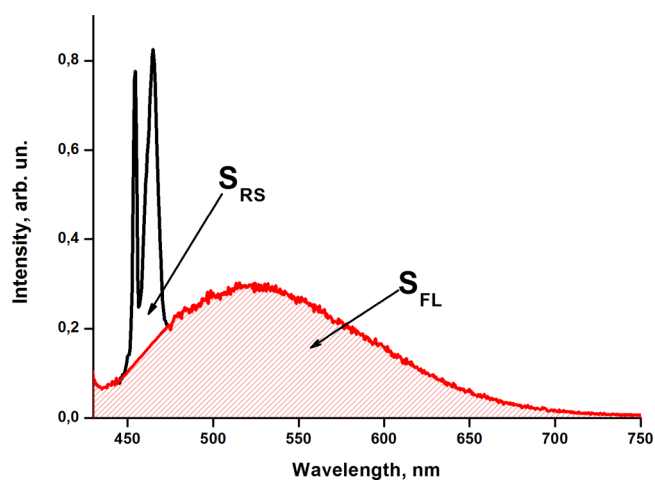


Figure 7. Fluorescence spectrum of DND-COOH in 40% water-ethanol solution. Illustration of calculation of F_0 .

intensity of stretching bands of OH and CH groups in water-ethanol suspensions of DND-COOH.

For measured spectra the dependence of parameter F_0 on the concentration of ethanol in the solvent was obtained (Figure 8). Our results demonstrated that the parameter F_0 of DND-COOH fluorescence in the suspensions increases with increase of ethanol concentration in the solvent (with the exception of the region of the concentration near 20%). In water-ethanol solution with concentration of ethanol below 20%, on the contrary the intensity of DND-COOH fluorescence shows a weak dependence on the ethanol fraction or slightly decreases.

As it was shown in the first part of the paper with the help of Raman spectroscopy, at room temperature DND-COOH are able to break the network of hydrogen bonds in water-ethanol solution with an ethanol concentration of 70%, an average energy of $|-16.2|$ kJ/mol, and the network of hydrogen bonds with an energy of $|-21.4|$ kJ/mol in water but nearly do not weaken hydrogen bonds with energy of $|-24.5|$ kJ/mol in water-ethanol solution with concentration of ethanol of 20%.

From these results, it is shown that the weaker and less dense the hydrogen bonds of the solvent are, the less impact they have on the fluorescence, that is, the weaker the solvent quenches the fluorescence of the DND-COOH. Thus, in water-ethanol suspensions by reducing the number of

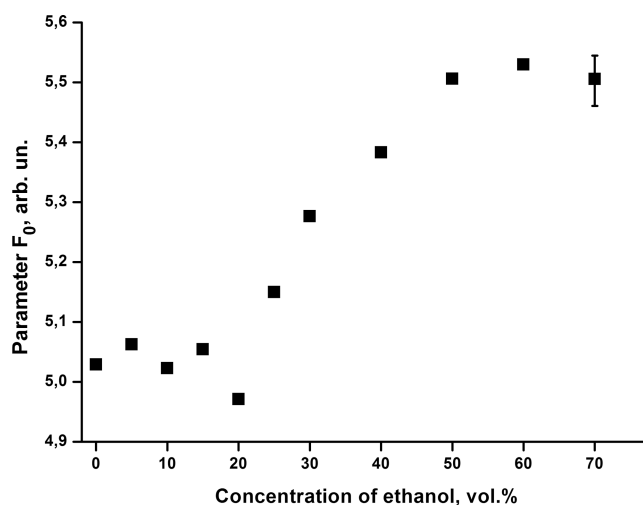


Figure 8. Dependence of fluorescence parameter F_0 DND-COOH on concentration of ethanol in water-ethanol solutions.

hydrogen bonds in suspensions compared to water, the influence of the hydrogen bonds on the surface of DND-COOH also decreases. However, in the water-ethanol suspensions with an ethanol content of 20% ethanol molecules are in semicathrate formations.^{47–50} This means that the surface of the DND-COOH interacts only with the water molecules (with strengthened hydrogen bonds compared to water up to $|-24.5|$ kJ/mol). Thus, in this case the number of hydrogen bonds in the surroundings of the nanoparticles is approximately the same as in water, but stronger hydrogen bonds cause weakening of the fluorescence (Figure 8). These results concerning the influence of the hydrogen bonds of solvent on DND-COOH fluorescence are in full agreement with the results obtained for DND-COOH and carbon dots in the other solvents with different strength hydrogen bonds.³⁵

Probably, disaggregation of DND-COOH in water-ethanol solution with ethanol concentration 70% increases by 4–5% (Table 1) the total surface “available” for solvent. It causes the decrease of the parameter F_0 in the range of ethanol concentration 60–70% (Figure 8).

According to the hypothesis suggested in the paper,⁴² mechanisms of DND fluorescence are caused by functional surface groups of DND. Authors assert that the red shift of the fluorescence in nanodiamonds and its excitation dependence are attributed to the joint effect of the relative changes of intensity of various types of oxygenous groups and some effects resulting from $n(\text{OH}) \rightarrow \pi^*(\text{CO})$ interactions between hydroxyl groups and carbonyl groups. Correspondingly, the fluorescence both dependent and independent of excitation can be obtained by designing the surface functional groups of nanodiamonds, which confirm the proposed mechanism. In general, fluorescence in nanodiamonds is produced in the processes of cooperation and competition of functional groups. Taking into account this hypothesis obtained results can be explained by the following. Hydrogen bond between oxygen atoms of surface group COO^- of DND and hydrogen atom of water molecule is formed due to donor-acceptor interaction. After absorption of radiation and excitation of group COO^- charge (electron), transfer from COO^- to water molecule occurs. The stronger the hydrogen bond is, the higher the probability of charge transfer is, and the stronger DND fluorescence quenching is.

CONCLUSIONS

In this study, the influence of dispersed DND-COOH and protic solvents on the properties of each other was established.

The temperature dependencies of bands of stretching vibrations of OH groups in water and water-ethanol solutions with the concentration of ethanol 20 and 70 vol % and suspensions of DND-COOH in the mentioned solvents were studied experimentally. Our observations show that the presence of DND-COOH significantly decreases the average energy of hydrogen bonds with initial average energy 1–21.41 kJ/mol (at room temperature) in water and water-ethanol solutions with the exception of the region of ethanol concentration 20%. However, DND-COOH cannot decrease the average energy of hydrogen bonds that are stronger than the hydrogen bonds in water by at least 1–31 kJ/mol.

The fluorescent properties of DND-COOH in the solvents with hydrogen bonds different by strength have been also investigated. It was found that the weaker the hydrogen bonds of the surrounding molecules of the solvent are, the more intense the fluorescence of dispersed DND-COOH is.

AUTHOR INFORMATION

Corresponding Author

*E-mail: tdolenko@lid.phys.msu.ru; tdolenko@mail.ru.

Notes

The authors declare no competing financial interest.

ACKNOWLEDGMENTS

The authors are thankful to Gary McGuire, International Technology Center, U.S.A., for valuable discussions. This study was supported by the grant of Russian Foundation for Basic Research (RFBF) No. 15-29-01290_ofi_m and No. 16-32-00882_mol; by the Russian Ministry of Science and Education Project (project ID RFMEFI60414X0082); by Russian Academy of Sciences, Program No.1; and by the Competitiveness Program of NRNU MEPhI.

REFERENCES

- (1) Krueger, A. New Carbon Materials: Biological Applications of Functionalized Nanodiamond Materials. *Chem. - Eur. J.* **2008**, *14*, 1382–1390.
- (2) Schrand, A. M.; Ciftan Hens, S. A.; Shenderova, O. A. Nanodiamonds Particles: Properties and Perspectives for Bioapplications. *Crit. Rev. Solid State Mater. Sci.* **2009**, *34* (1), 18–74.
- (3) Mochalin, V.; Shenderova, O.; Ho, D.; Gogotsi, Y. The Properties and Applications of Nanodiamonds. *Nat. Nanotechnol.* **2011**, *7* (1), 11–23.
- (4) Perevedentseva, E.; Cai, P.-J.; Chiu, Y.-C.; Cheng, C.-L. Characterizing Protein Activities on the Lysozyme and Nanodiamond Complex Prepared for Bio Applications. *Langmuir* **2011**, *27* (3), 1085–1091.
- (5) Chen, M.; Pierstorff, E. D.; Lam, R.; Li, S. Y.; Huang, H.; Osawa, E.; Ho, D. Nanodiamond-Mediated Delivery of Water-Insoluble Therapeutics. *ACS Nano* **2009**, *3* (7), 2016–2022.
- (6) Liu, K. K.; Zheng, W. W.; Wang, C. C.; Chiu, Y. C.; Cheng, C. L.; Lo, Y. S.; Chen, C.; Chao, J. I. Covalent Linkage of Nanodiamond-Paclitaxel for Drug Delivery and Cancer Therapy. *Nanotechnology* **2010**, *21*, 315106.
- (7) Lam, R.; Ho, D. Nanodiamonds as Vehicles for Systemic and Localized Drug Delivery. *Expert Opin. Drug Delivery* **2009**, *6* (9), 883–895.
- (8) von Haartman, E.; Jiang, H.; Khomich, A. A.; Zhang, J.; Burikov, S. A.; Dolenko, T. A.; Ruokolainen, J.; Gu, H.; Shenderova, O. A.; Vlasov, I. I.; Rosenholm, J. M. Core-Shell Designs of Photo-

luminescent Nanodiamonds with Porous Silica Coatings for Bioimaging and Drug Delivery I: Fabrication. *J. Mater. Chem. B* **2013**, *1* (18), 2358–2366.

(9) Prabhakar, N.; Nareoja, T.; von Haartman, E.; Karaman, D. S.; Jiang, H.; Koho, S.; Dolenko, T.; Hanninen, P.; Vlasov, D. I.; Ralchenko, V. G.; et al. Core-Shell Designs of Photoluminescent Nanodiamonds with Porous Silica Coatings for Bioimaging and Drug Delivery II: Application. *Nanoscale* **2013**, *5* (9), 3713–3722.

(10) Huang, L.-C. L.; Chang, H.-C. Adsorption and Immobilization of Cytochrome C on Nanodiamonds. *Langmuir* **2004**, *20* (14), 5879–5884.

(11) Dolenko, T. A.; Burikov, S. A.; Laptinskiy, K. A.; Laptinskaya, T. V.; Rosenholm, J. M.; Shiryayev, A. A.; Sabirov, A. R.; Vlasov, I. I. Study of Adsorption Properties of Functionalized Nanodiamonds in Aqueous Solutions of Metal Salts using Optical Spectroscopy. *J. Alloys Compd.* **2014**, *586*, S436–S439.

(12) Zobel, M.; Neder, R. B.; Kimber, S. A. J. Universal Solvent Restricting Induced by Colloidal Nanoparticles. *Science* **2015**, *347*, 292–294.

(13) Li, Y.; Chen, C.; Li, J.-T.; Yang, Y.; Lin, Z.-M. Surface Charges and Optical Characteristic of Colloidal Cubic SiC Nanocrystals. *Nanoscale Res. Lett.* **2011**, *6*, 454–461.

(14) Zakharko, Yu.; Botsoa, J.; Alekseev, S.; Lysenko, V.; Bluet, J.-M.; Marty, O.; Skryshevsky, V. A.; Guillot, G. Influence of the Interfacial Chemical Environment on the Luminescence of 3C - SiC Nanoparticles. *J. Appl. Phys.* **2010**, *107*, 013503.

(15) Lu, D.; Qiu, T.; Wu, L. Influence of Polar Solvent on Light-Emitting Property of SiO Nanoparticles Irradiated by Ultraviolet Ozone. *Eur. Phys. J. B* **2004**, *41* (1), 49–53.

(16) Antipov, A.; Bell, M.; Yasar, M.; Mitin, V.; Scharmach, W.; Swihart, M.; Verevkin, A.; Sergeev, A. Luminescence of Colloidal CdSe/ZnS Nanoparticles: High Sensitivity to Solvent Phase Transitions. *Nanoscale Res. Lett.* **2011**, *6*, 142–149.

(17) Wu, M.; Mukherjee, P.; Lamont, D. N.; Waldeck, D. H. Electron Transfer and Fluorescence Quenching of Nanoparticle Assemblies. *J. Phys. Chem. C* **2010**, *114*, 5751–5759.

(18) Wang, X.; Xu, S.; Xu, W. Synthesis of Highly Stable Fluorescent Ag Nanocluster - Polymer Nanoparticles in Aqueous Solution. *Nanoscale* **2011**, *3*, 4670–4675.

(19) Korobov, M.; Avramenko, N.; Bogachev, A.; Rozhkova, N.; Osawa, E. Nanophase of Water in Nano-Diamond Gel. *J. Phys. Chem. C* **2007**, *111* (20), 7330–7334.

(20) Avdeev, M.; Aksenov, V.; Rozhkova, N.; Garamus, V.; Willumeit, R.; Osawa, E. Aggregate Structure in Concentrated Liquid Dispersions of Ultrananocrystalline Diamond by Small-Angle Neutron Scattering. *J. Phys. Chem. C* **2009**, *113* (22), 9473–9479.

(21) Ozawa, M.; Inaguma, M.; Takahashi, M.; Kataoka, F.; Kruger, A.; Osawa, E. Preparation and Behavior of Brownish, Clear Nanodiamond Colloids. *Adv. Mater.* **2007**, *19*, 1201–1206.

(22) Neugart, F.; Zappe, A.; Jelezko, F.; Tietz, C.; Boudou, J. P.; Krueger, A.; Wrachtrup, J. Dynamics of Diamond Nanoparticles in Solution and Cells. *Nano Lett.* **2007**, *7* (12), 3588–3591.

(23) Hens, S.; Wallen, S.; Shenderova, O. Nanodiamond Fractional and the Products Thereof. U.S. Patent 7,569,205, August 4, 2009.

(24) Hu, S.; Sun, J.; Du, X.; Tian, F.; Jiang, L. The Formation of Multiply Twinning Structure and Photoluminescence of Well-Dispersed Nanodiamonds Produced by Pulsed-Laser Irradiation. *Diamond Relat. Mater.* **2008**, *17*, 142–146.

(25) Krueger, A.; Lang, D. Functionality is Key: Recent Progress in the Surface Functionalization of Nanodiamond. *Adv. Funct. Mater.* **2012**, *22*, 890–906.

(26) Gibson, N.; Shenderova, O.; Luo, T. J. M.; Moseenkov, S.; Bondar, V.; Puzyr, A.; Purtov, K.; Fitzgerald, Z.; Brenner, D. W. Colloidal Stability of Modified Nanodiamond Particles. *Diamond Relat. Mater.* **2009**, *18*, 620–626.

(27) Stehlik, S.; Glatzel, T.; Pichot, V.; Pawlak, R.; Meyer, E.; Spitzer, D.; Rezek, B. Water Interaction with Hydrogenated and Oxidized Detonation Nanodiamonds — Microscopic and Spectroscopic analyses. *Diamond Relat. Mater.* **2016**, *63*, 97–102.

- (28) Batsanov, S. S.; Lesnikov, E. V.; Dan'kin, D. A.; Balakhanov, D. M. Water Shells of Diamond Nanoparticles in Colloidal Solutions. *Appl. Phys. Lett.* **2014**, *104*, 133105.
- (29) Tomchuk, O. V.; Volkov, D. S.; Bulavin, L. A.; Rogachev, A. V.; Proskurnin, M. A.; Korobov, M. V.; Avdeev, M. V. Structural Characteristics of Aqueous Dispersions of Detonation Nanodiamond and Their Aggregate Fractions as Revealed by Small Angle Neutron Scattering. *J. Phys. Chem. C* **2015**, *119*, 794–802.
- (30) Chakrapani, V.; Angus, J. C.; Anderson, A. B.; Wolter, S. D.; Stoner, B. R.; Sumanasekera, G. U. Charge Transfer Equilibria Between Diamond and an Aqueous Oxygen Electrochemical Redox Couple. *Science* **2007**, *318*, 1424–1430.
- (31) Petit, T.; Girard, H. A.; Trouvé, A.; Batonneau-Gener, I.; Bergonzo, P.; Arnault, J.-C. Surface Transfer Doping Can Mediate Both Colloidal Stability and Self-Assembly of Nanodiamonds. *Nanoscale* **2013**, *5*, 8958–8962.
- (32) Petit, T.; Pflüger, M.; Tolksdorf, D.; Xiao, J.; Aziz, E. F. Valence Holes Observed in Nanodiamonds Dispersed in Water. *Nanoscale* **2015**, *7*, 2987–2991.
- (33) Petit, T.; Yuzawa, H.; Nagasaka, M.; Yamanoi, R.; Osawa, E.; Kosugi, N.; Aziz, E. F. Probing Interfacial Water on Nanodiamonds in Colloidal Dispersion. *J. Phys. Chem. Lett.* **2015**, *6*, 2909–2912.
- (34) Dolenko, T. A.; Burikov, S. A.; Rosenholm, J. M.; Shenderova, O. A.; Vlasov, I. I. Diamond-Water Coupling Effects in Raman and Photoluminescence Spectra of Nanodiamond Colloidal Suspensions. *J. Phys. Chem. C* **2012**, *116*, 24314–24319.
- (35) Dolenko, T. A.; Burikov, S. A.; Laptinskiy, K. A.; Rosenholm, J. M.; Shenderova, O. A.; Vlasov, I. I. Evidence of Carbon Nanoparticles – Solvent Molecules Interactions in Raman and Fluorescence Spectra. *Phys. Status Solidi A* **2015**, *212* (11), 2512–2518.
- (36) Chaplin, M. Water Structure and Science. http://www1.lsbu.ac.uk/water/water_structure_science.html (accessed March 4, 2016).
- (37) Walrafen, G. E. Raman Studies of the Effects of Temperature on Water and Electrolyte Solutions. *J. Chem. Phys.* **1966**, *44* (4), 1546–1558.
- (38) Walrafen, G. E.; Fisher, M. R.; Hokmabadi, M. S.; Yang, W.-H. Temperature Dependence of the Low- and High-Frequency Raman Scattering from Liquid Water. *J. Chem. Phys.* **1986**, *85* (12), 6970–6982.
- (39) Dolenko, T. A.; Churina, I. V.; Fadeev, V. V.; Glushkov, S. M. Valence Band of Liquid Water Raman Scattering: Some Peculiarities and Applications in the Diagnostics of Water Media. *J. Raman Spectrosc.* **2000**, *31*, 863–870.
- (40) Gogolinskaia, T. A.; Patsaeva, S. V.; Fadeev, V. V. The Regularities of Change of the 3100–3700 cm⁻¹ Band of Water Raman Scattering in Salt Aqueous Solutions. *Dokl. Akad. Nauk. SSSR+* **1986**, *290* (5), 1099–1103.
- (41) Dolenko, T. A.; Burikov, S. A.; Dolenko, S. A.; Efitorov, A. O.; Mirgorod, Y. A. Raman Spectroscopy of Micellization-Induced Liquid-Liquid Fluctuations in Sodium Dodecyl Sulfate Aqueous Solutions. *J. Mol. Liq.* **2015**, *204*, 44–49.
- (42) Xiao, J.; Liu, P.; Li, L.; Yang, G. Fluorescence Origin of Nanodiamonds. *J. Phys. Chem. C* **2015**, *119* (4), 2239–2248.
- (43) Liu, K.-K.; Cheng, C.-L.; Chang, C.-C.; Chao, J.-I. Biocompatible and Detectable Carboxylated Nanodiamond on Human Cell. *Nanotechnology* **2007**, *18* (32), 325102.
- (44) Shenderova, O.; Panich, A. M.; Moseenkov, S.; Hens, S. C.; Kuznetsov, V.; Vieth, H.-M. Hydroxylated Detonation Nanodiamond: FTIR, XPS, and NMR Studies. *J. Phys. Chem. C* **2011**, *115*, 19005–19011.
- (45) Shenderova, O.; Koscheev, A.; Zaripov, N.; Petrov, I.; Skryabin, Y.; Detkov, P.; Turner, S.; Van Tendeloo, G. Surface Chemistry and Properties of Ozone-Purified Detonation Nanodiamonds. *J. Phys. Chem. C* **2011**, *115*, 9827.
- (46) Turner, S.; Lebedev, O. I.; Shenderova, O.; Vlasov, I. I.; Verbeeck, J.; Van Tendeloo, G. Determination of Size, Morphology, and Nitrogen Impurity Location in Treated Detonation Nanodiamond by Transmission Electron Microscopy. *Adv. Funct. Mater.* **2009**, *19*, 2116–2124.
- (47) Mizuno, K.; Miyashita, Y.; Shindo, Y.; Ogawa, H. NMR and FT-IR Studies of Hydrogen Bonds in Ethanol-Water Mixtures. *J. Phys. Chem.* **1995**, *99* (10), 3225–3228.
- (48) Nishi, N.; Takahashi, S.; Matsumoto, M.; Tanaka, A.; Muraya, K.; Takamuku, T.; Yamaguchi, T. Hydrogen-Bonded Cluster Formation and Hydrophobic Solute Association in Aqueous Solutions of Ethanol. *J. Phys. Chem.* **1995**, *99* (1), 462–468.
- (49) Wakisaka, A.; Matsuura, K. Microheterogeneity of Ethanol-Water Binary Mixtures Observed at the Cluster Level. *J. Mol. Liq.* **2006**, *129* (1–2), 25–32.
- (50) Burikov, S.; Dolenko, T.; Patsaeva, S.; Starokurov, Yu.; Yuzhakov, V. Raman and IR Spectroscopy Research on Hydrogen Bonding in Water-Ethanol Systems. *Mol. Phys.* **2010**, *108* (18), 2427–2436.
- (51) Yang, D.; Wang, H. Effects of Hydrogen Bonding on the Transition Properties of Ethanol–Water Clusters: A TD-DFT Study. *J. Cluster Sci.* **2013**, *24*, 485–495.
- (52) Dolenko, T. A.; Burikov, S. A.; Dolenko, S. A.; Efitorov, A. O.; Plastinin, I. V.; Yuzhakov, V. I.; Patsaeva, S. V. Raman Spectroscopy of Water-Ethanol Solutions: the Estimation of Hydrogen Bonding Energy and the Evidence of Clathrate-like Structures. *J. Phys. Chem. A* **2015**, *119* (44), 10806–10815.